Diabetologia (2015) 58:384–392
DOI 10.1007/s00125-014-3438-y

ARTICLE

Genetic deletion of *Wdr13* improves the metabolic phenotype of *Lepr*$^{db/db}$ mice by modulating AP1 and PPARγ target genes

Vijay P. Singh · Chandrashekaran Gurunathan · Sachin Singh · Bhavtaran Singh · B. Jyothi Lakshmi · Arun P. Mishra · Satish Kumar

Received: 12 August 2014 / Accepted: 15 October 2014 / Published online: 23 November 2014

Abstract
Aim/hypothesis Type 2 diabetes is a complex disease characterised by hyperglycaemia, hyperinsulinaemia, dyslipidaemia and insulin resistance accompanied by inflammation. Previously, we showed that mice lacking the *Wdr13* gene had increased islet mass due to enhanced beta cell proliferation. We hypothesised that introgression of a *Wdr13*-null mutation, a beta cell-proliferative phenotype, into *Lepr*$^{db/db}$ mice, a beta cell-destructive phenotype, might rescue the diabetic phenotype of the latter.
Methods Wdr13-deficient mice were crossed with *Lepr*$^{db/db}$ mice to generate mice with the double mutation. We measured various serum metabolic variables of *Wdr13*$^{+/0}$*Lepr*$^{db/db}$ and *Wdr13*$^{-/0}$*Lepr*$^{db/db}$ mice. Further, we analysed the histopathology and gene expression of peroxisome proliferator-activated receptor (PPAR)γ and, activator protein (AP)1 targets in various metabolic tissues.
Results Lepr$^{db/db}$ mice with the *Wdr13* deletion had a massively increased islet mass, hyperinsulinaemia and adipocyte hypertrophy. The increase in beta cell mass in *Wdr13*$^{-/0}$ *Lepr*$^{db/db}$ mice was due to an increase in beta cell proliferation. Hypertrophy of adipocytes may be the result of increase in transcription of *Pparg* and its target genes, leading in turn to increased expression of several lipogenic genes. We also observed a significant decrease in the expression of AP1 and nuclear factor κ light chain enhancer of activated B cells (NFκB) target genes involved in inflammation.
Conclusions/interpretation This study provides evidence that loss of WD repeat domain 13 (WDR13) protein in the *Lepr*$^{db/db}$ mouse model of diabetes is beneficial. Based on these findings, we suggest that WDR13 may be a potential drug target for ameliorating hyperglycaemia and inflammation in diabetic conditions.

Keywords AP1 · Diabetes · Islets · Leptin receptor · PPAR · Wdr13

Abbreviations

AP	Activator protein
CCMB	Centre for Cellular and Molecular Biology
GTT	Glucose tolerance test
H&E	Haematoxylin and eosin
HRP	Horseradish peroxidase
IκBα	Nuclear factor of κ light polypeptide gene enhancer in B cells inhibitor α
ITT	Insulin tolerance test
JNK	c-Jun N-terminal kinase
NFκB	Nuclear factor kappa-light-chain-enhancer of activated B cells
PPAR	Peroxisome proliferator-activated receptor
qRT-PCR	Quantitative RT-PCR
WDR13	WD repeat domain 13

Vijay P. Singh and Chandrashekaran Gurunathan contributed equally to this study.

Electronic supplementary material The online version of this article (doi:10.1007/s00125-014-3438-y) contains peer-reviewed but unedited supplementary material, which is available to authorised users.

V. P. Singh · C. Gurunathan · S. Singh · B. Singh · B. J. Lakshmi · A. P. Mishra · S. Kumar
National Facility for Transgenic and Gene Knockout Mice, Council of Scientific and Industrial Research-Centre for Cellular and Molecular Biology, Habsiguda, Hyderabad, India

Present address:
S. Kumar (✉)
National Institute of Animal Biotechnology,
1-121/1, 4th and 5th Floor Axis Clinicals Building,
Miyapur, Hyderabad 500 049, India
e-mail: satishk@niab.org.in

Introduction

Type 2 diabetes is a worldwide disease, estimated to affect more than 340 million people, with approximately 3.4 million associated deaths per year [1]. Type 2 diabetes is associated with increases in obesity, insulin resistance, inflammation and pancreatic beta cell malfunction [2, 3]. Insulin resistance is one of the main reasons for beta cell failure in animal models of type 2 diabetes and in humans [4]. The increase in obesity and the resulting insulin resistance initially trigger beta cell expansion. However, long-term insulin resistance leads to beta cell stress and, ultimately, beta cell failure [5]. Beta cell mass and function are also regulated by a variety of adipokines, namely leptin, adiponectin, resistin and visfatin secreted from adipose tissue [6].

The leptin receptor mutant (*Lepr*$^{db/db}$) mouse is a model of type 2 diabetes. The mutant mice show hyperphagia due to defects in leptin signalling, which leads to obesity, hyperglycaemia, hyperinsulinaemia, dyslipidaemia, insulin resistance and inflammation at around 3 months [7]. Glucotoxicity and lipotoxicity are two secondary phenomena implicated in the pathology of type 2 diabetes, resulting from excessive glucose and/or lipids. Glucotoxicity occurs via dysregulation of genes involved in gluconeogenesis, glycogenolysis and glycolysis: glucose 6-phosphate, phosphoenolpyruvate carboxykinase (PEPCK), glycogen phosphorylase and glucokinase in liver [8, 9]. Lipotoxicity occurs via impaired hepatic fatty acid metabolism and adipose tissue dysfunction [10]. Obesity is accompanied by a chronic low-grade inflammation in adipose tissue and liver characterised by infiltration of cytokines, chemokines and macrophages together with activation of pro-inflammatory transcription factors such as activator protein (AP)1, nuclear factor κ light chain enhancer of activated B cells (NFκB) and 5′ UTR regulatory element (PU.1) [11, 12].

WDR13 is a member of the WD repeats protein family and occurs in most tissues, being abundant in the pancreas, brain, testis and ovary [13, 14]. *Wdr13*-knockout mice have increased pancreatic beta cell proliferation, which leads to increased islet mass, hyperinsulinaemia and better glucose clearance, notwithstanding mild obesity at a later age [15]. We hypothesised that introgression of a *Wdr13*-null mutation, a beta cell-proliferative phenotype, into *Lepr*$^{db/db}$ mice, a beta cell-destructive phenotype, might rescue the diabetic phenotype of the latter. Here, we show that the deletion of *Wdr13* gene in *Lepr*$^{db/db}$ mice significantly reduces circulating blood glucose and inflammation.

Methods

Generation of mice and metabolic measurements The Institutional Animal Ethics Committee of the Centre for Cellular and Molecular Biology (CCMB) approved all animal experiments. To generate congenic *Wdr13*-knockout C57BL/6J mice (JAX mice, Bar Harbor, ME, USA), CD1 *Wdr13*-knockout mice were backcrossed for nine generations. To generate double heterozygotes for *Wdr13* and *Lepr* mutant alleles, *Wdr13*-heterozygous females were mated with heterozygous males of the B6.BKS-*Lepr*^{db} strain (JAX mice, Bar Harbor, ME, USA [stock 000697]). Finally, double-heterozygous male and female mice obtained from this cross were bred to generate mice with the double mutation in the *Wdr13* and *Lepr* genes. Animals were genotyped using PCR. Body weight, food intake, glucose and insulin tolerance testing and insulin measurements were performed as described previously [15]. Circulating triacylglycerol was measured using the glycerol-3-phosphate oxidase/phenol+aminophenazone (GPO/PAP) method (Coral Clinical Systems, Goa, India). For triacylglycerol content, frozen liver (~50 mg) was homogenised in 500 μl PBS and chloroform-extracted lipids were dried using a Speedvac and re-dissolved in isopropanol. Triacylglycerol was quantified in 96 well plates. NEFA were measured using a half micro test kit (Roche, Basel, Switzerland).

Histology western blot analysis and real-time PCR Histology and western blot analysis were performed as described [15]. All the tissues for histology, western blot and real-time PCR analyses were collected from mice fasted for 16 h. Haematoxylin and eosin (H&E) staining and immunostaining were carried out on 4 μm sections, mounted on positively charged slides, from tissues fixed overnight in 4% paraformaldehyde and embedded in paraffin. Immunostaining was performed using antibodies to jun proto-oncogene (c-Jun) ([sc-45] Santa Cruz Biotechnology, Paso Robles, CA, USA), Ki-67 ([AB9260] EMD Millipore, Billerica, MA, USA) and Mac-2 (also known as galectin-3) ([CL8942AP] Cedarlane Labs, ON, Canada). Antibodies to c-Jun and Ki-67 were detected using a biotin–streptavidin–horseradish peroxidase (HRP) system and Mac-2 was detected using an HRP-conjugated antibody and developed with diaminobenzidine (DAB) substrate ([11718096001] Roche). Positive cells were counted manually using Axioskop (AxioVision software, www.zeiss.co.in/microscopy/en_in/downloads/axiovision.html). A minimum of 1,000 beta cells was considered for the quantification of each group. For Oil Red O (Sigma-Aldrich, Bangalore, India) staining, liver tissues were frozen in OCT compound (Sigma-Aldrich) and 8 μm sections were mounted on slides and stained with 0.5% Oil Red O solution. Western blots were performed using antibodies to nuclear factor of κ light polypeptide gene enhancer in B cells inhibitor, alpha (IκBα) ([4812S] Cell Signaling Technology, Beverly, MA, USA), c-Jun, p-c-Jun ([sc-822] Santa Cruz Biotechnology) and β-actin ([ab8226] Abcam, Tokyo, Japan). Total RNA was extracted from frozen tissues using an RNeasy mini kit

(Qiagen, Limburg, the Netherlands). Reverse transcription was performed using ImProm II Reverse Transcriptase kit (Promega, Madison, WI, USA). Quantitative (q)RT-PCR was performed using Ex Taq Sybr Green (Takara, New Delhi, India). Primer sequences are presented in electronic supplementary material (ESM) Table 1.

Apoptotic assay Tissue sections were prepared as described previously [15]. TUNEL assays were performed using the DeadEnd Fluorometric TUNEL System (Promega). Confocal images were recorded and TUNEL-positive beta cells were counted manually from a total of 5–6 mice per genotype.

Pparg promoter reporter assay The *Pparg* promoter was cloned in pGL3 (Promega) according to Zhu et al [16].

Statistical analysis The unpaired Student's *t* test was used, with significance at $p < 0.05$. Data are represented as mean± SEM.

Results

$Wdr13^{-/0}Lepr^{db/db}$ mice resist weight loss We measured the body weights of $Wdr13^{-/0}Lepr^{db/db}$ and $Lepr^{db/db}$ mice to 6 months of age. $Wdr13^{-/0}Lepr^{db/db}$ mice weighed less than $Lepr^{db/db}$ mice at 3 months (Fig. 1a). In $Lepr^{db/db}$ mice there was no difference in body weight at 3 and 6 months whereas $Wdr13^{-/0}Lepr^{db/db}$ showed a steady increase in body weight throughout the experiment to 6 months (Fig. 1b). This difference between these two genotypes was attributable to a significant loss in body weight in $Lepr^{db/db}$ mice after 4 months of age owing to diabetic complications, whereas $Wdr13^{-/0}Lepr^{db/db}$ mice showed significant body weight gain from 4 to 6 months (Fig. 1c). No significant difference in food intake was observed between these two genotypes (Fig. 1d).

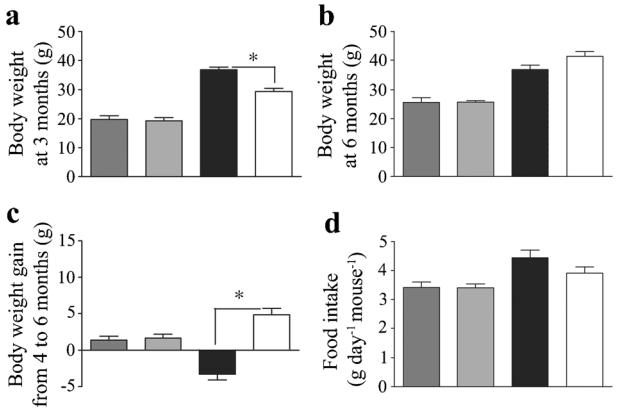

Fig. 1 The effect of *Wdr13* gene deletion on body weight and food intake in $Lepr^{db/db}$ mice. (**a**, **b**) Body weight measurements taken at (**a**) 3 and (**b**) 6 months. (**c**) The weight gain was calculated as the difference in body weight at 4 and 6 months (**d**) Feed consumption of various genotypes. n=6–8 mice per group. Dark grey bars, $Wdr13^{+/0}Lepr^{+/+}$ mice; light grey bars, $Wdr13^{-/0}Lepr^{+/+}$ mice; black bars, $Wdr13^{+/0}Lepr^{db/db}$ mice; white bars, $Wdr13^{-/0}Lepr^{db/db}$ mice. *p<0.05

$Wdr13^{-/0}Lepr^{db/db}$ mice showed improved metabolic phenotype and better glucose tolerance To understand the effect of *Wdr13* deletion, we measured glucose, insulin, triacylglycerol and NEFA in $Wdr13^{-/0}Lepr^{db/db}$ and $Lepr^{db/db}$ mice and the respective control genotypes. Fasting and fed blood glucose levels were significantly lower in $Wdr13^{-/0}Lepr^{db/db}$ mice than in $Lepr^{db/db}$ mice at both 3 and 6 months (Fig. 2a–d). Interestingly, at 3 months, the insulin levels were comparable in these two genotypes (Fig. 2e, g). $Lepr^{db/db}$ mice were already diabetic whereas $Wdr13^{-/0}Lepr^{db/db}$ mice had a significantly lower glucose level than $Lepr^{db/db}$ mice. As expected, the insulin level in $Lepr^{db/db}$ mice at 6 months was lower than that at 3 months because of the destruction of beta cells, whereas in the $Wdr13^{-/0}Lepr^{db/db}$ mice insulin level continued to increase (Fig. 2e–h) and that was reflected in the glucose values. In addition to reduced blood glucose, serum triacylglycerol was also significantly lower in $Wdr13^{-/0}Lepr^{db/db}$ mice at 6 months (Fig. 2j). Similarly, NEFA was significantly lower in $Wdr13^{-/0}Lepr^{db/db}$ than in $Lepr^{db/db}$ mice at this age (Fig. 2l).

The glucose tolerance test (GTT) showed no significant difference in glucose clearance between $Wdr13^{-/0}Lepr^{db/db}$ and $Lepr^{db/db}$ mice at 3 months (Fig. 3a) except for a significantly low basal glucose level in $Wdr13^{-/0}Lepr^{db/db}$ mice as already described above (Fig. 2a). At 6 months, $Wdr13^{-/0}Lepr^{db/db}$ mice cleared glucose efficiently, restoring to basal values after 120 min, while $Lepr^{db/db}$ mice showed severely impaired glucose tolerance as reflected by glucose levels of >55.5 mmol/l, even at 120 min (Fig. 3b). Insulin tolerance test at 3 months showed better insulin sensitivity in $Wdr13^{-/0}Lepr^{db/db}$ mice compared with $Lepr^{db/db}$ mice, the former showing compromised insulin sensitivity when compared with wild type (Fig. 3c). At 6 months we observed insulin resistance in $Wdr13^{-/0}Lepr^{db/db}$ mice even though the basal glucose level was significantly lower than in $Lepr^{db/db}$ mice (Fig. 3d).

$Wdr13^{-/0}Lepr^{db/db}$ mice have greater islet area To understand the effect of *Wdr13* gene deletion in $Lepr^{db/db}$ mice, we examined the pancreatic histology. At 3 months there was no difference in islet area between $Lepr^{db/db}$ and $Wdr13^{-/0}Lepr^{db/db}$ mice (ESM Fig. 1c, d) whereas it was significantly higher in the $Wdr13^{-/0}Lepr^{db/db}$ mice at 6 months (Fig. 4a). Moreover, the islet boundaries were well defined and the islets appeared healthier in the $Wdr13^{-/0}Lepr^{db/db}$ mice. Thus, improved glucose clearance in $Wdr13^{-/0}Lepr^{db/db}$ mice might be due to the increase in the islet area.

$Wdr13^{-/0}Lepr^{db/db}$ mice have increased beta cell proliferation We assayed beta cell proliferation in $Wdr13^{-/0}Lepr^{db/db}$ mice

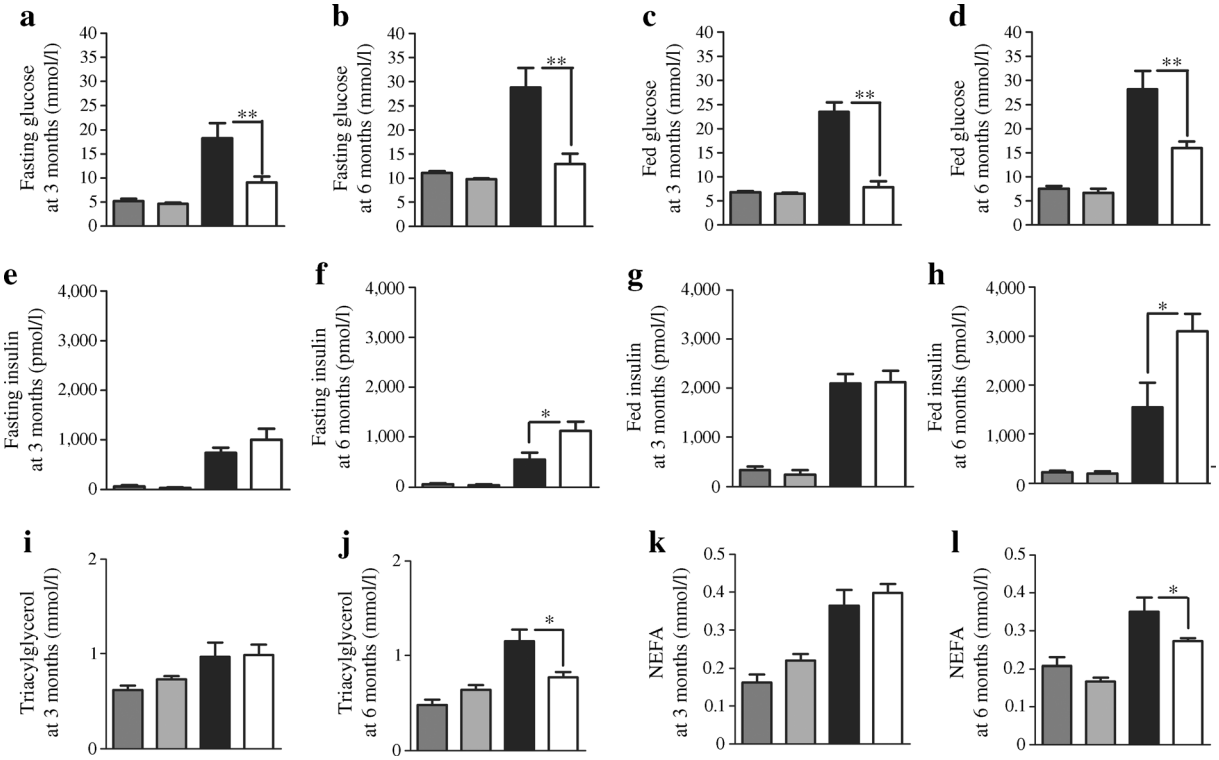

Fig. 2 The effect of *Wdr13* gene deletion on metabolic variables in $Lepr^{db/db}$ mice at 3 and 6 months. Blood glucose levels after 16 h of fasting (**a**, **b**) and in the random fed state (**c**, **d**). Serum insulin levels after 16 h of fasting (**e**, **f**) and in the random fed state (**g**, **h**). (**i**, **j**) Serum triacylglycerol after 16 h of fasting. (**k**, **l**) Serum NEFA after 16 h of fasting. n=5–8 mice per group. Dark grey bars, $Wdr13^{+/0}Lepr^{+/+}$ mice; light grey bars, $Wdr13^{-/0}Lepr^{+/+}$ mice; black bars, $Wdr13^{+/0}Lepr^{db/db}$ mice; white bars, $Wdr13^{-/0}Lepr^{db/db}$ mice. *p< 0.05 and **p< 0.01

using Ki-67 antibody. The number of Ki-67-positive cells was twofold higher (p=0.07) in $Wdr13^{-/0}Lepr^{db/db}$ mice than in $Lepr^{db/db}$ mice at 6 months (Fig. 4b). Therefore, the increase in islet area may be attributed to the increase in beta cell proliferation in $Wdr13^{-/0}Lepr^{db/db}$. We did not observe any difference in the number of apoptotic beta cells using TUNEL assay in the genotypes at 3 months (ESM Fig. 1a, b). It was difficult to find any apoptotic cells at 6 months in $Lepr^{db/db}$ mice as there were only disintegrated and damaged islets and it was not possible to compare the extent of apoptosis.

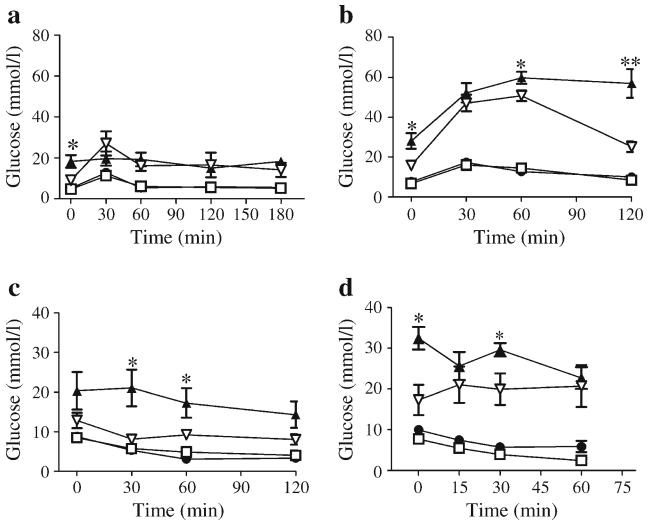

Fig. 3 The effect of *Wdr13* gene deletion on glucose clearance and insulin sensitivity in $Lepr^{db/db}$ mice. GTT at (**a**) 3 and (**b**) 6 months. ITT at (**c**) 3 and (**d**) 6 months. n=5–8 mice per group. Circles, $Wdr13^{+/0}Lepr^{+/+}$ mice; squares, $Wdr13^{-/0}Lepr^{+/+}$ mice; triangles, $Wdr13^{+/0}Lepr^{db/db}$ mice; inverted triangles, $Wdr13^{-/0}Lepr^{db/db}$ mice. *p< 0.05 and **p<0.01

$Wdr13^{-/0}Lepr^{db/db}$ mice showed reduced triacylglycerol in liver and hypertrophy of adipocytes Liver histology at 6 months showed a drastic reduction in lipid droplets in $Wdr13^{-/0}Lepr^{db/db}$ mice compared with $Lepr^{db/db}$ mice (Fig. 4c). Analysis of liver triacylglycerol content further confirmed the reduced lipid accumulation in $Wdr13^{-/0}Lepr^{db/db}$ mice (Fig. 4c). Histological examination of epididymal fat pad sections revealed hypertrophy of adipocytes in both the $Lepr^{db/db}$ and $Wdr13^{-/0}Lepr^{db/db}$ mice (Fig. 4d). However, $Wdr13^{-/0}Lepr^{db/db}$ mice showed more hypertrophy with compact and regular adipocyte morphology, in contrast to $Lepr^{db/db}$ mice.

$Wdr13^{-/0}Lepr^{db/db}$ mice showed reduced pancreatic inflammation WDR13 acts as a transcriptional activator of c-Jun in the presence of high c-Jun N-terminal kinase (JNK) activity (V. P. Singh, S. Katta, S. Kumar, unpublished data) and c-Jun regulates many AP1 and NFκB target genes. JNK signalling promotes insulin resistance in beta cells [17]. c-Jun immunostaining in beta cells showed reduced levels in

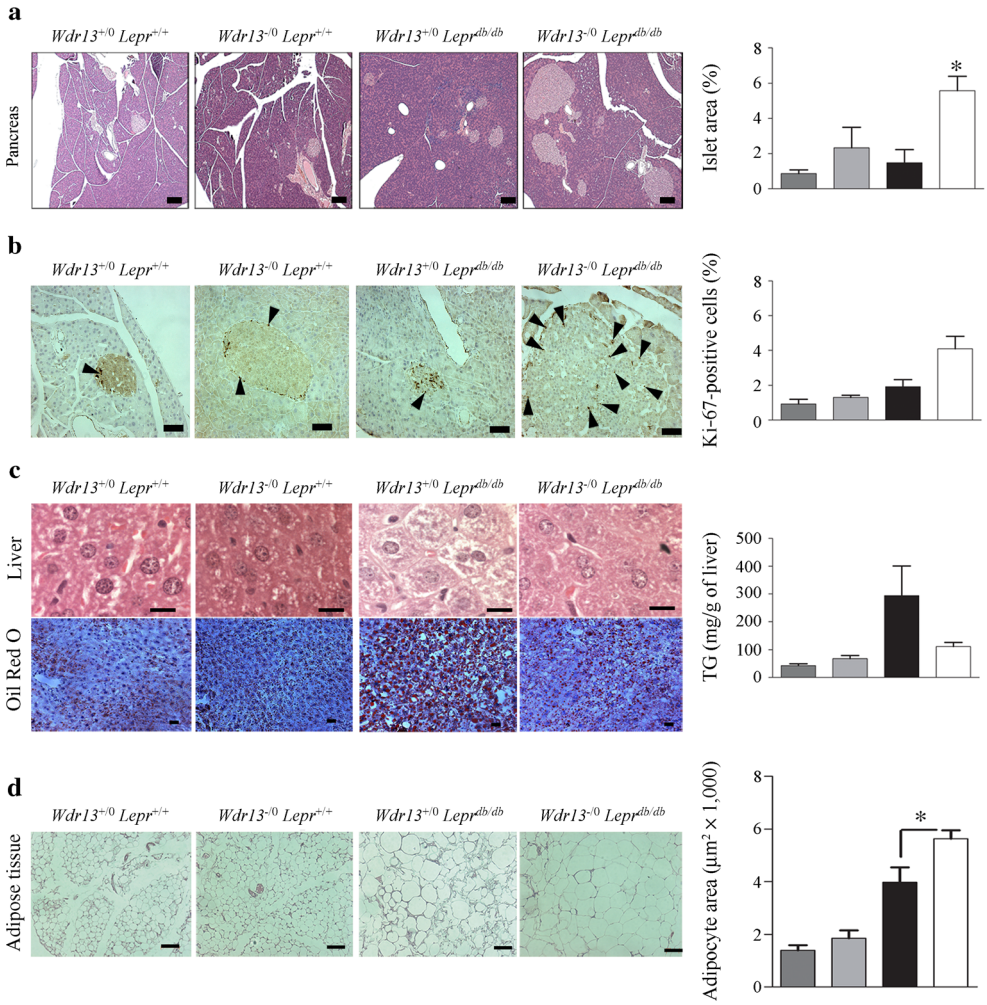

Fig. 4 The effect of *Wdr13* deletion on the histology of pancreas, liver and adipose tissue in $Lepr^{db/db}$ mice at 6 months. (**a**) H&E staining of the pancreas with quantification of islet area. Scale bars, 100 μm. (**b**) Immunostaining for Ki-67-positive cells (arrowheads). Scale bars, 50 μm. (**c**) Liver H&E and Oil Red O staining. Scale bars, 10 μm and 20 μm (n=5 mice per group). (**d**) H&E staining of the epididymal fat pad. Scale bars, 100 μm. Dark grey bars, $Wdr13^{+/0}Lepr^{+/+}$ mice; light grey bars, $Wdr13^{-/0}Lepr^{+/+}$ mice; black bars, $Wdr13^{+/0}Lepr^{db/db}$ mice; white bars, $Wdr13^{-/0}Lepr^{db/db}$ mice. *p< 0.05

$Wdr13^{-/0}Lepr^{db/db}$ mice (Fig. 5a). In addition, analysis of inflammatory markers such as *Emr1* (macrophage) and *Mcp-1* (also known as *Ccl2*) in total pancreatic extracts showed reduced expression in $Wdr13^{-/0}Lepr^{db/db}$ mice (Fig. 5b).

Improved adipose tissue function in $Wdr13^{-/0}Lepr^{db/db}$ *mice* Adipose tissue gene expression analysis showed a consistent increase in *Acc1* (also known as *Acaca*), *Acc2* (also known as *Acacb*), *Fasn*, *Srebp1c* (also known as *Srebf1*) and *Scd1* in $Wdr13^{-/0}Lepr^{db/db}$ mice, indicating increased lipogenesis and improved fat-accumulation capacity of adipocytes (Fig. 6a). As PPARγ is the master regulator of adipose tissue function, and adipose tissue functions are correlated mainly with its transcription factors, we examined the expression of *Pparg* and its target genes. A significant—approximately 20-fold—increase in *Pparg* mRNA level was observed in $Wdr13^{-/0}$ mice compared with wild type. Similarly, $Wdr13^{-/0}Lepr^{db/db}$ mice showed twofold increase in *Pparg* expression in contrast to $Lepr^{db/db}$ (Fig. 6b). As expected, there was also an increase in the expression of its target genes, *Ap2* (also known as *Fabp4*),

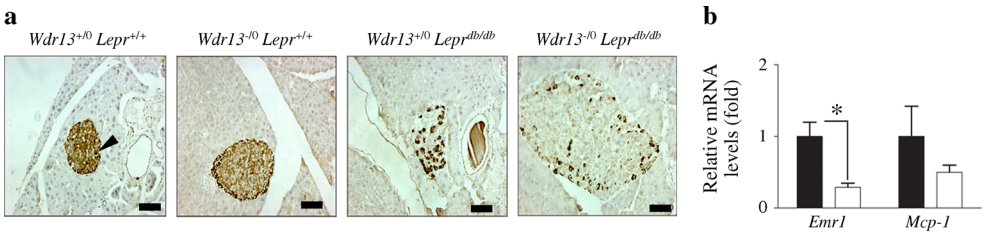

Fig. 5 The effect of *Wdr13* deletion on pancreatic inflammation. (**a**) c-Jun immunostaining of the pancreas. Scale bars, 50 μm. (**b**) mRNA levels of genes involved in inflammation. Expression has been calculated relative to $Wdr13^{+/0}Lepr^{db/db}$ mice, set at 1. Black bars, $Wdr13^{+/0}Lepr^{db/db}$ mice; white bars, $Wdr13^{-/0}Lepr^{db/db}$ mice. *p< 0.05

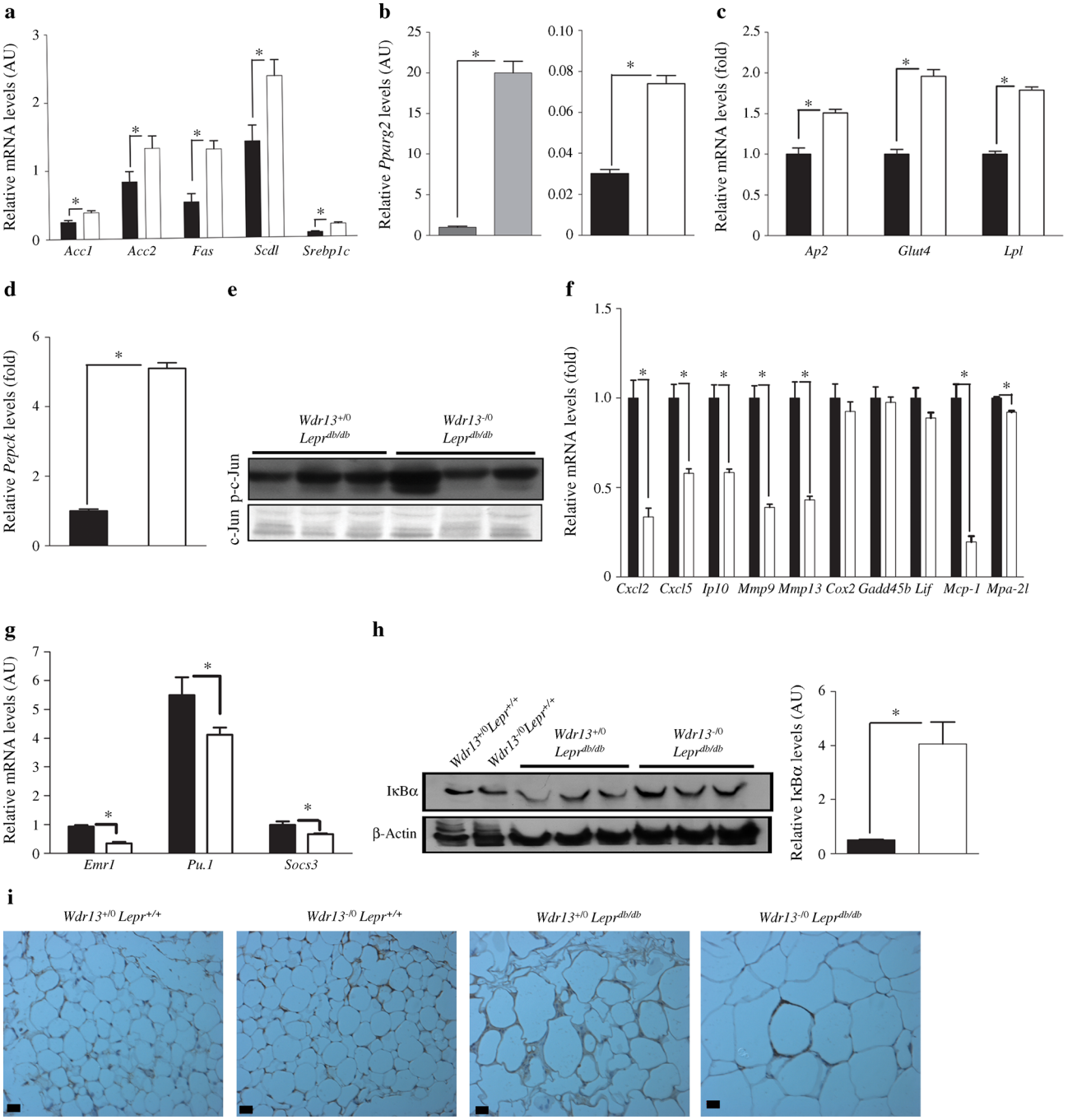

Fig. 6 The effect of *Wdr13* deletion on adipose tissue lipogenesis and inflammation in $Lepr^{db/db}$ mice at 6 months. (**a**) mRNA levels of genes involved in lipid metabolism. (**b**) qRT-PCR for *Pparg*. (**c**) mRNA levels of PPARγ target genes. (**d**) *Pepck* mRNA levels in adipose tissue. (**e**) Western blot for phosphorylated and total c-Jun levels. (**f**) mRNA levels of AP1 and NFκB target genes. (**g**) mRNA levels of genes involved in inflammation. (**h**) Western blot for IκBα in adipose tissue. B-actin was used as loading control. (**i**) Mac-2 staining for macrophages. *Ip10* is also known as *Cxcl10*; *Mpa-2l* is also known as *Gbp6*. In (**c**), (**d**) and (**f**) expression has been calculated relative to $Wdr13^{+/0}Lepr^{db/db}$ mice, set at 1. Scale bars, 20 μm. Dark grey bars, $Wdr13^{+/0}Lepr^{+/+}$ mice; light grey bars, $Wdr13^{-/0}Lepr^{+/+}$ mice; black bars, $Wdr13^{+/0}Lepr^{db/db}$ mice; white bars, $Wdr13^{-/0}Lepr^{db/db}$ mice. n=6 mice per group. *p< 0.05

Glut4 and *Lpl* (Fig. 6c). In $Wdr13^{-/0}Lepr^{db/db}$ mice, we observed a fourfold increase in mRNA levels of *Pepck-c* (also known as *Pck1*) compared with $Lepr^{db/db}$ (Fig. 6d), consistent with a reduction in circulating NEFA (Fig. 2l), as reported earlier, which suggests increased de novo glyceroneogenesis.

$Wdr13^{-/0}Lepr^{db/db}$ mice showed reduced inflammation in adipose tissue As mentioned above, *Wdr13* acts as a transcriptional activator of c-Jun and it is known that $Lepr^{db/db}$ mice have high JNK activity and high p-c-Jun level, which activate AP1-specific pro-inflammatory target genes. Western blot data showed similar

levels of p-c-Jun in *Lepr*$^{db/db}$ and *Wdr13*$^{-/0}$*Lepr*$^{db/db}$ mice (Fig. 6e). Thus, we analysed the expression of inflammatory genes in the *Wdr13*$^{-/0}$*Lepr*$^{db/db}$ mice. In adipose tissue, in spite of increased hypertrophy in *Wdr13*$^{-/0}$*Lepr*$^{db/db}$ mice, a decrease in inflammatory markers such as *Emr1*, *Socs*3 and the transcription factor *Pu.1* along with AP1 and NFκB target genes containing AP1 sites was observed compared with *Lepr*$^{db/db}$ (Fig. 6f, g). As *Wdr13*$^{-/0}$*Lepr*$^{db/db}$ mice showed decreased expression of NFκB target genes we analysed the protein levels of IκBα. In *Wdr13*$^{-/0}$*Lepr*$^{db/db}$ mice IκBα levels were significantly higher than in *Lepr*$^{db/db}$, implying a reduction in inflammation through retention of NFκB by IκBα in the cytoplasm as NFκB–IκBα complex (Fig. 6h). Mac-2 staining for the accumulation of macrophages around adipose tissue displayed less crown-like structure (CLS) formation in *Wdr13*$^{-/0}$*Lepr*$^{db/db}$ mice (Fig. 6i).

Next, we studied the expression of genes involved in the major pathways of glucose and fatty acid metabolism in liver. *Wdr13*$^{-/0}$*Lepr*$^{db/db}$ mice showed a significant decrease in the expression of key gluconeogenic enzyme pyruvate dehydrogenase kinase, isozyme 4 (PDK4) and lipogenic enzymes Fas (TNF receptor superfamily member 6) (FAS) and stearoyl-coenzyme A desaturase 1 (SCD1), whereas increased expression of acetyl-coenzyme A carboxylase α (ACC) and diacylglycerol O-acyltransferase 2 (DGAT2) was observed (ESM Fig. 2b). The liver inflammatory genes *Emr1* and *Socs3* were also downregulated in the *Wdr13*$^{-/0}$*Lepr*$^{db/db}$ mice compared with *Lepr*$^{db/db}$ (ESM Fig. 2b). Furthermore, the presence of intact IκBα protein (ESM Fig. 2a) and reduced protein levels of p-c-Jun (ESM Fig. 2c) were consistent with the reduced expression of inflammatory genes in the livers of *Wdr13*$^{-/0}$*Lepr*$^{db/db}$ mice.

Discussion

We show that deletion of *Wdr13* in *Lepr*$^{db/db}$ mice significantly reduces levels of circulating blood glucose and NEFA. We observed that, compared with *Lepr*$^{db/db}$, *Wdr13*$^{-/0}$*Lepr*$^{db/db}$ mice had higher beta cell proliferation, massively increased islet mass, and hyperinsulinaemia, accompanied by better glucose clearance. *Wdr13*$^{-/0}$*Lepr*$^{db/db}$ mice displayed improved adipose tissue function via increased PPARγ and expression of its downstream target genes. These mice were protected from obesity-induced inflammation by reduced expression of AP1- and NFκB-induced target genes.

Lepr$^{db/db}$ mice gain weight rapidly till about 3 months, and then progressively lose body weight because of severe impairment of glucose and lipid metabolism [7]. In the absence of *Wdr13*, *Lepr*$^{db/db}$ mice had lower body weight at 3 months (Fig. 1a). The lower body weight of the *Wdr13*$^{-/0}$*Lepr*$^{db/db}$ mice might have been a reflection of a lower birthweight of *Wdr13*-knockout mice [15], or *Wdr13* deletion per se might have prevented body weight gain in the *Wdr13*$^{-/0}$*Lepr*$^{db/db}$ mice from birth to 3 months. Beyond 3 months, the *Wdr13*$^{-/0}$*Lepr*$^{db/db}$ mice continued to increase in body weight till the termination of the experiment at 6 months, in contrast to *Lepr*$^{db/db}$ mice. These data were consistent with the significantly improved glucose homeostasis observed in the absence of *Wdr13* in *Lepr*$^{db/db}$ mice.

Diabetes in *Lepr*$^{db/db}$ mice is characterised by hyperinsulinaemia, hyperglycaemia, obesity and insulin resistance [7]. At 3 months *Wdr13*$^{-/0}$*Lepr*$^{db/db}$ and *Lepr*$^{db/db}$ mice showed similar insulin levels (Fig. 2e, g). Interestingly, glucose levels were significantly reduced in the *Wdr13*$^{-/0}$*Lepr*$^{db/db}$ mice, indicating better insulin sensitivity in the absence of *Wdr13* in *Lepr*$^{db/db}$, which was further confirmed by insulin tolerance test (ITT) at 3 months (Fig. 3c). However, *Wdr13*$^{-/0}$*Lepr*$^{db/db}$ mice were still hyperglycaemic and insulin resistant when compared with wild type (Figs 2a, c and 3c). Further, at 6 months *Lepr*$^{db/db}$ mice showed severe hyperglycaemia along with a reduction in insulin levels, as expected, because of beta cell destruction [4]. However, insulin levels were higher in the *Wdr13*$^{-/0}$*Lepr*$^{db/db}$ mice. The effect of this increase in insulin level was reflected in better glucose clearance in *Wdr13*$^{-/0}$*Lepr*$^{db/db}$ mice than in *Lepr*$^{db/db}$ mice. At 6 months *Wdr13*$^{-/0}$*Lepr*$^{db/db}$ mice did not respond to exogenous insulin in contrast to *Lepr*$^{db/db}$ mice (Fig. 3d). This difference might reflect the very high levels of endogenous insulin levels intrinsic to *Wdr13*$^{-/0}$*Lepr*$^{db/db}$ mice. As ITT makes a limited contribution to an understanding of insulin resistance in a tissue-specific manner, the possibility remains that insulin resistance may vary in different tissues and adipose tissue insulin sensitivity in *Wdr13*$^{-/0}$*Lepr*$^{db/db}$ mice might have improved. A continuous demand for insulin in *Lepr*$^{db/db}$ mice leads to pancreatic beta cell death [4]. As there is no change in the number of apoptotic beta cells in *Wdr13*$^{-/0}$*Lepr*$^{db/db}$ mice compared with *Lepr*$^{db/db}$ (ESM Fig. 1a) and WDR13 is a negative regulator of pancreatic beta cell proliferation [15], the hyperinsulinaemia in the *Wdr13*$^{-/0}$*Lepr*$^{db/db}$ mice is primarily due to the increased islet mass resulting from the pancreatic beta cell proliferation, as shown by Ki-67 staining (Fig. 4a, b). These results are consistent with our previous studies on the role of *Wdr13* in beta cell proliferation [15].

In liver, insulin suppresses gluconeogenesis and increases lipogenesis [8, 18], whereas in adipose tissue it promotes glucose and fatty acid uptake [19], and suppresses lipolysis [20]. PPARγ plays a crucial role in the control of glucose and lipid homeostasis [21–26]. We found that the *Wdr13*$^{-/0}$*Lepr*$^{db/db}$ mice had a significant increase in mRNA levels of *Pparg* and its downstream target genes, *Glut4* (also known as *Slc2a4*), *Lpl* and *Ap2* (also known as *Fabp4*) (Fig. 6b, c). The *Wdr13*$^{-/0}$*Lepr*$^{db/db}$ mice showed increased expression of lipogenic genes such as

Acc1, *Acc2*, *Fasn*, *Scd1* and *Srebp1c* in adipose tissue in comparison with $Lepr^{db/db}$ mice, indicating increased lipogenesis (Fig. 6a). These data are consistent with the adipose tissue hypertrophy seen in $Wdr13^{-/0}Lepr^{db/db}$ mice (Fig. 4d). It appears that the increased lipogenesis may be one of the contributing factors responsible for lowering the glucose levels, notwithstanding higher insulin levels, for the maintenance of glucose homeostasis. *Wdr13* is expressed in adipocytes and our data support the cell-autonomous role of *Wdr13* in adipocytes as shown by enhanced adipocyte lipogenesis in the absence of *Wdr13*. It is very likely that the increased insulin levels in *Wdr13*-knockout animals would reduce lipolysis in adipose tissue, resulting in increased fat storage. To delineate the relative contribution of these two possible mechanisms for an increase in fat accumulation in adipocytes, one would need a tissue-specific knockout of *Wdr13* gene. Previous studies have shown that genetic deletion of adipose tissue chaperones increased de novo lipogenesis in adipose tissue, rendering the mice resistant to metabolic syndrome [27–30]. The enhanced lipogenesis in adipose tissue of $Wdr13^{-/0}Lepr^{db/db}$ mice was complemented by a reduction in lipolysis, as shown by lower levels of triacylglycerol and NEFA in serum compared with $Lepr^{db/db}$ [31, 32]. In the livers of $Wdr13^{-/0}Lepr^{db/db}$ mice, the picture from Oil Red O staining and triacylglycerol content was clearly of a reduction in lipogenesis (Fig. 4c). To understand this reduction, we analysed the mRNA levels of six lipogenic genes and that of the transcription factor sterol regulatory element binding transcription factor 1 (SREBP1C). With the exception of *Acc1* and *Acc2*, the genes showed downregulation. It is possible that downregulation of FAS, which catalyses the downstream step of *Acc1/Acc2* in fatty acid synthesis, may contribute to the reduction in de novo lipogenesis [33]. The upregulation of *Acc1* and *Acc2* observed by us at the mRNA level is an apparent contradiction of the $Wdr13^{-/0}Lepr^{db/db}$ phenotype. It is known that the activities of these two enzymes are not only regulated at the transcription level but also through post-translational modification, specifically phosphorylation [34]. Further investigations are needed to resolve this.

Type 2 diabetes and obesity have been associated with chronic low-grade inflammation [11, 35]. Consistent with the improved functionality of adipose tissue and other metabolic variables in the $Wdr13^{-/0}Lepr^{db/db}$ mice, a significant reduction was observed in inflammatory markers (Fig. 6g) and macrophage infiltration (Fig. 6i) in these mice. Similarly, inflammation was reduced in the pancreas and liver of $Wdr13^{-/0}Lepr^{db/db}$ mice (Fig. 5 and ESM Fig. 2b), demonstrating a systemic effect due to reduced adipose tissue inflammation. The intact IκBα in the $Wdr13^{-/0}Lepr^{db/db}$ mice further strengthens our proposition that inflammation is reduced in various metabolic tissues of these mice (Fig. 6h and ESM Fig. 2a). A parallel study showed that *Wdr13* interacts with c-Jun and acts as a transcriptional co-activator in the presence of high JNK activity in various cell types (V. P. Singh, S. Katta, S. Kumar, unpublished data). It is established that $Lepr^{db/db}$ mice and other mouse models of diabetes exhibit high JNK activity due to inflammation. Analysis of AP1 and NFκB target genes containing AP1 sites showed reduced expression in $Wdr13^{-/0}Lepr^{db/db}$ mice (Figs 5b and 6f and ESM Fig. 2), strengthening the above findings. *Wdr13* is expressed in various metabolic tissues: pancreatic islets, liver, adipose and muscle [15]. It is possible that the reduced expression of AP1 target genes (pro-inflammatory) in these tissues may also contribute to the beneficial effect of loss of WDR13. The *Pparg* promoter contains an AP1 site and WDR13 binds with c-Jun. Promoter analysis of *Pparg2* in 3T3L1 cells showed a significant increase after *c-Jun* overexpression (ESM Fig. 3), suggesting an interesting and indirect role of *Wdr13* in *Pparg2* regulation. However, at present we do not understand the regulation of *Pparg2* promoter by WDR13 in the presence of high JNK activity.

In conclusion, we examined in detail the phenotype of pancreas, liver and adipose tissue using whole-body *Wdr13* knockout and provide evidence of a beneficial effect of loss of this protein in $Lepr^{db/db}$ mice. Interestingly, our data suggest that inflammation is reduced in the pancreas, liver and adipose tissue as a result of the downregulation of AP1-target genes in these tissues. Given the expression of *Wdr13* in multiple tissues including brain, tissue-specific knockout of this gene will further help in explaining the phenotype we describe.

Acknowledgements We thank A. Raj (CCMB, Hyderabad, India) for his technical assistance in histology and N. Rangaraj (CCMB, Hyderabad, India) for assistance in microscopy. We thank A. B. Siva for critical reading of the manuscript and suggestions, and L. Singh for support.

Funding The Department of Biotechnology (DBT), Government of India, New Delhi and the Council of Scientific and Industrial Research (CSIR), New Delhi supported this research.

Contribution statement All authors were responsible for the conception and design, or analysis and interpretation of data; and drafting the article or revising it critically for important intellectual content. All authors gave final approval of the version to be published. Satish Kumar is the guarantor of this work and, as such, had full access to all the data in the study and takes responsibility for the integrity of the data and the accuracy of the data analysis.

Duality of interest The authors confirm that there is no duality of interest associated with this manuscript.

References

1. Roglic G, Unwin N, Bennett PH et al (2005) The burden of mortality attributable to diabetes: realistic estimates for the year 2000. Diabetes Care 28:2130–2135
2. Brownlee M (2005) The pathobiology of diabetic complications: a unifying mechanism. Diabetes 54:1615–1625
3. Wajchenberg BL (2007) Beta-cell failure in diabetes and preservation by clinical treatment. Endocr Rev 28:187–218

4. Prentki M, Nolan CJ (2006) Islet beta cell failure in type 2 diabetes. J Clin Invest 116:1802–1812
5. Robertson R, Zhou H, Zhang T, Harmon JS (2007) Chronic oxidative stress as a mechanism for glucose toxicity of the beta cell in type 2 diabetes. Cell Biochem Biophys 48:139–146
6. Dunmore SJ, Brown JE (2013) The role of adipokines in beta-cell failure of type 2 diabetes. J Endocrinol 216:T37–T45
7. Sharma K, McCue P, Dunn SR (2003) Diabetic kidney disease in the db/db mouse. Am J Physiol Renal Physiol 284:F1138–F1144
8. Postic C, Dentin R, Girard J (2004) Role of the liver in the control of carbohydrate and lipid homeostasis. Diabetes Metab 30:398–408
9. Matschinsky FM, Magnuson MA, Zelent D et al (2006) The network of glucokinase-expressing cells in glucose homeostasis and the potential of glucokinase activators for diabetes therapy. Diabetes 55:1–12
10. Lewis GF, Carpentier A, Adeli K, Giacca A (2002) Disordered fat storage and mobilization in the pathogenesis of insulin resistance and type 2 diabetes. Endocr Rev 23:201–229
11. Xu H, Barnes GT, Yang Q et al (2003) Chronic inflammation in fat plays a crucial role in the development of obesity-related insulin resistance. J Clin Invest 112:1821–1830
12. Gregor MF, Hotamisligil GS (2011) Inflammatory mechanisms in obesity. Annu Rev Immunol 29:415–445
13. Singh BN, Suresh A, UmaPrasad G et al (2003) A highly conserved human gene encoding a novel member of WD-repeat family of proteins (WDR13). Genomics 81:315–328
14. Suresh A, Shah V, Rani DS et al (2005) A mouse gene encoding a novel member of the WD family of proteins is highly conserved and predominantly expressed in the testis (Wdr13). Mol Reprod Dev 72: 299–310
15. Singh VP, Lakshmi BJ, Singh S et al (2012) Lack of Wdr13 gene in mice leads to enhanced pancreatic beta cell proliferation, hyperinsulinemia and mild obesity. PLoS One 7:e38685
16. Zhu Y, Qi C, Korenberg JR et al (1995) Structural organization of mouse peroxisome proliferator-activated receptor gamma (mPPAR gamma) gene: alternative promoter use and different splicing yield two mPPAR gamma isoforms. Proc Natl Acad Sci U S A 92:7921–7925
17. Lanuza-Masdeu J, Arevalo MI, Vila C, Barbera A, Gomis R, Caelles C (2013) In vivo JNK activation in pancreatic beta-cells leads to glucose intolerance caused by insulin resistance in pancreas. Diabetes 62:2308–2317
18. Muoio DM, Newgard CB (2008) Mechanisms of disease: molecular and metabolic mechanisms of insulin resistance and beta-cell failure in type 2 diabetes. Nat Rev Mol Cell Biol 9:193–205
19. Girard J, Perdereau D, Foufelle F, Prip-Buus C, Ferre P (1994) Regulation of lipogenic enzyme gene expression by nutrients and hormones. FASEB J 8:36–42
20. Bergman RN, Ader M (2000) Free fatty acids and pathogenesis of type 2 diabetes mellitus. Trends Endocrinol Metab 11:351–356
21. Medina-Gomez G, Gray SL, Yetukuri L et al (2007) PPAR gamma 2 prevents lipotoxicity by controlling adipose tissue expandability and peripheral lipid metabolism. PLoS Genet 3:e64
22. Miles PD, Barak Y, He W, Evans RM, Olefsky JM (2000) Improved insulin-sensitivity in mice heterozygous for PPAR-gamma deficiency. J Clin Invest 105:287–292
23. Kubota N, Terauchi Y, Miki H et al (1999) PPAR gamma mediates high-fat diet-induced adipocyte hypertrophy and insulin resistance. Mol Cell 4:597–609
24. He W, Barak Y, Hevener A et al (2003) Adipose-specific peroxisome proliferator-activated receptor gamma knockout causes insulin resistance in fat and liver but not in muscle. Proc Natl Acad Sci U S A 100:15712–15717
25. Kim HS, Hwang YC, Koo SH et al (2013) PPAR-gamma activation increases insulin secretion through the up-regulation of the free fatty acid receptor GPR40 in pancreatic beta-cells. PLoS One 8:e50128
26. Ferre P (2004) The biology of peroxisome proliferator-activated receptors: relationship with lipid metabolism and insulin sensitivity. Diabetes 53(Suppl 1):S43–S50
27. Cao H, Gerhold K, Mayers JR, Wiest MM, Watkins SM, Hotamisligil GS (2008) Identification of a lipokine, a lipid hormone linking adipose tissue to systemic metabolism. Cell 134:933–944
28. Kuriyama H, Liang G, Engelking LJ, Horton JD, Goldstein JL, Brown MS (2005) Compensatory increase in fatty acid synthesis in adipose tissue of mice with conditional deficiency of SCAP in liver. Cell Metab 1:41–51
29. Waki H, Park KW, Mitro N et al (2007) The small molecule harmine is an antidiabetic cell-type-specific regulator of PPARgamma expression. Cell Metab 5:357–370
30. Maeda K, Cao H, Kono K et al (2005) Adipocyte/macrophage fatty acid binding proteins control integrated metabolic responses in obesity and diabetes. Cell Metab 1:107–119
31. Magkos F, Fabbrini E, Conte C, Patterson BW, Klein S (2012) Relationship between adipose tissue lipolytic activity and skeletal muscle insulin resistance in nondiabetic women. J Clin Endocrinol Metab 97:E1219–E1223
32. Mittelman SD, Bergman RN (2000) Inhibition of lipolysis causes suppression of endogenous glucose production independent of changes in insulin. Am J Physiol Endocrinol Metab 279:E630–E637
33. Strable MS, Ntambi JM (2010) Genetic control of de novo lipogenesis: role in diet-induced obesity. Crit Rev Biochem Mol Biol 45: 199–214
34. Fullerton MD, Galic S, Marcinko K et al (2013) Single phosphorylation sites in Acc1 and Acc2 regulate lipid homeostasis and the insulin-sensitizing effects of metformin. Nat Med 19:1649–1654
35. Galic S, Fullerton MD, Schertzer JD et al (2011) Hematopoietic AMPK beta1 reduces mouse adipose tissue macrophage inflammation and insulin resistance in obesity. J Clin Invest 121:4903–4915